

**Weak Turbulence Theory of
Ion Temperature Gradient Modes
for
Inverted Density Plasmas**

T. S. Hahm and W. M. Tang

**Princeton Plasma Physics Laboratory
Princeton University
Princeton, New Jersey 08543**

Abstract

Typical profiles measured in H-mode ("high confinement") discharges from tokamaks such as JET [*Proceedings of the 15th European Conference on Controlled Fusion and Plasma Heating* (European Physical Society, Budapest, 1988), Vol. 12B, Part 1, p. 2239] and DIII-D [Phys. Fluids **31**, 3738 (1988)] suggest that the ion temperature gradient instability threshold parameter η_i ($\equiv d \ln T_i / d \ln n_i$) could be negative in many cases. Previous linear theoretical calculations [Phys. Fluids B **1**, 1185 (1989)] have established the onset conditions for these negative η_i -modes and the fact that their growth rate is much smaller than their real frequency over a wide range of negative η_i values. This has motivated the present nonlinear weak turbulence analysis to assess the relevance of such instabilities for confinement in H-mode plasmas. The nonlinear eigenmode equation indicates that the 3-wave coupling to shorter wavelength modes is the dominant nonlinear saturation mechanism. It is found that both the saturation level for these fluctuations and the magnitude of the associated ion thermal diffusivity are considerably smaller than the strong turbulence mixing length type estimates for the more conventional positive- η_i -instabilities.

DISCLAIMER

This report was prepared as an account of work sponsored by an agency of the United States Government. Neither the United States Government nor any agency thereof, nor any of their employees, makes any warranty, express or implied, or assumes any legal liability or responsibility for the accuracy, completeness, or usefulness of any information, apparatus, product, or process disclosed, or represents that its use would not infringe privately owned rights. Reference herein to any specific commercial product, process, or service by trade name, trademark, manufacturer, or otherwise does not necessarily constitute or imply its endorsement, recommendation, or favoring by the United States Government or any agency thereof. The views and opinions of authors expressed herein do not necessarily state or reflect those of the United States Government or any agency thereof.

1. Introduction

The possible role of ion temperature gradient instabilities in influencing the enhanced confinement properties in H-mode plasmas¹⁻³ has been an active topic in tokamak transport studies.⁴⁻⁸ Motivated by the observations of profiles in JET^{1,2} and DIII-D³ H-mode discharges which suggest that the parameter η_i could be negative in many cases, recent theoretical work has established the onset conditions and general linear properties of these negative η_i -modes.⁷ The fact that the growth rate was found to be much smaller than the real frequency over a wide range of negative η_i values⁷ has encouraged the present development of a weak turbulence nonlinear theory to determine the confinement consequences of these instabilities.

In this paper, a nonlinear eigenmode equation is derived in the weak turbulence regime from the nonlinear gyrokinetic equation,⁹ including both three-wave decay type mode coupling and ion Compton scattering (wave-wave-particle interaction) processes. Unlike recent weak turbulence studies of positive η_i modes near threshold,¹⁰ the present work deals with the *nonlocal* nature of the radial eigenmode structure using a nonlinear eigenmode equation in a multi-rational surface sheared slab geometry. The dominant nonlinear term in the equation which leads to the saturation of the fluctuations is found to be the coherent mode coupling to weakly stable shorter poloidal wavelength modes. Our results indicate that both the saturation level for these fluctuations and the magnitude of the associated ion thermal diffusivity are considerably smaller than the strong turbulence

mixing length type estimates for the more conventional positive- η_i -instabilities.

The organization of the paper is as follows. In Sec. II, the appropriate linear theory governing the threshold conditions and eigenmode structure for η_i instabilities is presented. Beginning with the formal analysis of Ref. 7, we proceed here to derive the detailed properties of negative- η_i -modes near threshold. The weak turbulence nonlinear theory determining the nonlinear evolution of these instabilities is developed in Sec. III. Saturation levels for the fluctuations and the associated ion thermal transport are calculated in Sec. IV. Here it is demonstrated that the present results indicate significantly lower levels of transport than the usual strong-turbulence mixing length type estimates. The implications of these conclusions for H-mode plasma confinement are discussed in Sec. V.

II. Linear Theory

In this section, we present the linear analysis of ion temperature gradient drift modes with attention focused on those properties which help justify the application of weak turbulence theory. Included are the derivations of the threshold condition for negative- η_i -modes, the real frequency and growth rate of these instabilities near threshold, and their characteristic radial mode structure. The theoretical model studied here consists of the Boltzmann electron response and collisionless gyrokinetic ion response in a sheared slab geometry where the magnetic field is given by $\mathbf{B} = B_0(\mathbf{z} + \mathbf{y}\mathbf{x}/L_S)$. For the negative η_i cases of interest, previous work⁷ has

demonstrated that the fluid approximation, $\omega \gg k_{\parallel} v_{ti}$ can be effectively utilized to calculate the ion density response. Imposing the quasi-neutrality condition, we can write the following eigenmode equation,¹¹

$$\{ \tau^{-1} + 1 - (1 - \omega_{*i}/\omega)\Gamma_0 + (\omega_{*i}/\omega)\eta_i b(\Gamma_1 - \Gamma_0) \} \psi + (v_{ti} k_{\parallel}/\omega)^2 [(1 - \omega_{*i}/\omega)\eta_i \{ \Gamma_0 + b(\Gamma_1 - \Gamma_0) \} - (1 - \omega_{*i}/\omega)\Gamma_0] \psi = 0, \quad (1)$$

where $\omega_{*i} = (cT_i k_y / eB_0) d \ln n_0 / dx$, $\eta_i = d \ln T_i / d \ln n_0$, $v_{ti}^2 = T_i / M_i$, $\tau = T_e / T_i$, $k_x^2 = -\partial^2 / \partial x^2$, $b = \rho_i^2 (k_x^2 + k_y^2) = b_x + b_y$, $\Gamma_n = e^{-b} I_n(b)$, ψ is the perturbed electrostatic potential, and I_n is a modified Bessel function.

In carrying out the analysis, we consider long to moderate perpendicular wavelength modes with $b < 1$. This is motivated by reasons of simplicity as well as the fact that toroidal curvature modifications to the sheared slab results are relatively minor in this range.¹² After expanding Γ_0 and Γ_1 to first order in b_x and then in b_y for each term, we obtain the following second order differential equation,

$$\{ (1 + (1 + \eta_i) / \Omega \tau) - (1 + (1 + 2\eta_i) / \Omega \tau) 3b_y / 2 \} \partial^2 \psi / \partial X^2 + \{ 1 / \Omega - 1 - \tau b_y (1 + (1 + \eta_i) / \Omega) \} \psi + \{ (1 + (1 + \eta_i) / \Omega \tau) - (1 + (1 + 2\eta_i) / \Omega \tau) b_y \} (L_n / L_s)^2 (X / \Omega)^2 \psi = 0, \quad (2)$$

where $\Omega = \omega_{*e} / \omega$, $\omega_{*e} = -\tau \omega_{*i}$, $L_n^{-1} = -d \ln n_0 / dx$, and X has been normalized to $\rho_s = \tau^{1/2} \rho_i$, i.e., $X = x / \rho_s$.

Note here that we retain the finite Larmor radius corrections to the ion acoustic term and to the polarization drift (terms usually ignored in previous studies¹³). Although they are small in magnitude, these terms nevertheless strongly affect the wavelength-dependence of the threshold condition. This wavelength-dependence of threshold is crucial for nonlinear considerations because it will indicate the range of the spectrum most

easily excited.

Since Eq.(2) is the familiar Weber equation, the following dispersion relation is easily obtained for the lowest radial harmonic.

$$\Omega\{(1+b_S)\Omega-1+b_y(1+\eta_i)\} = i(L_N/L_S)\{\Omega+(1+\eta_i)/\tau-b_y(\Omega+(1+2\eta_i)/\tau)\}^{1/2} \{ (1+(1+\eta_i)/\Omega\tau) - (1+(1+2\eta_i)/\Omega)3b_y/2\}^{1/2}\Omega^{1/2}, \quad (3)$$

where $b_S = \tau b_y$. This dispersion relation is more complicated than the commonly adopted form¹³ because of the aforementioned b_y corrections to the right side of Eq.(3). Since Ω should be real at marginal stability, both sides of Eq.(3) vanish. Hence, from the left side of this equation, we obtain

$$\Omega_r = \{1-b_y(1+\eta_i)\}/(1+b_S). \quad (4)$$

The other root at $\Omega = 0$ violates the fluid approximation and does not lead to the correct threshold value. From the right side of Eq.(3) together with Eq.(4), we obtain the threshold values,

$$\eta_{c1} = - (1+\tau)(1+b_y), \quad (5a)$$

and
$$\eta_{c2} = - (1+\tau)(1+3b_y/2). \quad (5b)$$

More accurate analysis including higher order terms is needed to obtain a unique threshold value. Since both formulas have the same trend (increasing in magnitude as b_y is increased) and do not differ significantly in magnitude, we will not pursue this refinement.

We next proceed to derive the growth rate near threshold by treating the right side of Eq.(3) perturbatively; i.e.,

$$\begin{aligned} \text{Im}(\Omega) &= [\tau(1+b_S)\{1-b_y(1+\eta_i)\}L_S/L_N]^{-1} \\ & (1-5b_y/2)(\eta_i-\eta_{c1})^{1/2}(\eta_i-\eta_{c2})^{1/2}. \end{aligned} \quad (6)$$

Note that the last two factors of Eq.(6) indicate instability for

$|\eta_i| > |\eta_{c2}|$ and marginally stable (neutral) modes for $\eta_{c1} > \eta_i > \eta_{c2}$. In

this sense, η_{c2} is the more relevant threshold. Comparing with Eq.(4), one clearly sees that the first factor in Eq.(6) ensures that the trend $|\omega_r| \gg \delta$ is satisfied even away from marginal stability for finite b_s . This trend is consistent with numerical results from previous work.⁷ It should be remembered that a more stringent condition for the applicability of the weak turbulence expansion is $|\delta\omega| \gg \delta$, where $\delta\omega = \omega - \omega_{pe}$. This is due to the fact that when $\delta\omega = 0$, one can find a poloidally rotating frame with $v_\theta = \rho_s C_s / L_n$, where the mode can be considered as a purely growing instability. To address this issue we return to Eq.(4) to obtain $\delta\omega = -b_s(1+\tau+\eta_i)\omega_{pe}/(1+b_s)\tau$. Using Eq.(6), we find

$$|\delta/\delta\omega| = |L_n/L_s|(1-5b_y/2) [b_s\{1-b_y(1+\eta_i)\}]^{-1} \{(\eta_i - \eta_{c1})(\eta_i - \eta_{c2})\}^{1/2} / |1+\tau+\eta_i|. \quad (7a)$$

Therefore, $|\delta\omega| \gg \delta$ is satisfied near the threshold. To demonstrate that this is also true away from threshold, consider $|\eta_i - \eta_{c2}| \gg 1$. The expression in the last bracket $\{ \}$ of Eq. (7a) can then be approximated by unity, thereby leading to the result,

$$|\delta/\delta\omega| = |L_n/L_s|(1-5b_y/2) [b_s\{1-b_y(1+\eta_i)\}]^{-1}. \quad (7b)$$

This indicates that $|\delta\omega| \gg \delta$ is always satisfied for $b_s > |L_n/L_s|$. For the nearly flat density profile cases where $|L_n| \rightarrow L_s$, the condition becomes less stringent since the $b_y\eta_i$ term in the denominator of Eq. (7b) is significant. Therefore, we expect the weak turbulence expansion scheme to be valid for a wide range of negative η_i values. The values for δ and $\delta\omega$ as well as their ratio from Eq.(7a) are plotted in Fig.1.

The radial mode structure can also be easily obtained from Eq.(2):
i.e.,

$$\psi \propto \exp(-X^2/2\Delta^2)$$

where $\Delta = |L_S \Omega / L_n|^{1/2}$ is the radial mode width. Here we ignore higher radial eigenmodes for simplicity. Although these modes can have larger growth rates in specific parameter regimes away from the threshold,^{14,15} they are also generally more susceptible to stabilizing kinetic modifications.¹⁶

III. Weak Turbulence Nonlinear Theory

The procedure for calculating the nonlinear saturation of fluctuations associated with negative η_i instabilities is developed here using the weak turbulence expansion scheme.¹⁷ Although the more conventional approach has been to employ the wave kinetic equation to obtain the saturation level of these instabilities,^{17,18} we find it more efficient to solve the nonlinear eigenmode equation, which allows us to retain the nonlocal radial structure of the fluctuations. The dominant nonlinear saturation mechanism has been found to be the coherent mode coupling to weakly stable shorter wavelength modes. This is because the ion Compton scattering is negligible for the moderately long ($|L_n/L_S| < b_S \ll 1$) wavelength modes which are most easily excited. As will be shown later, the frequency matching condition, $\omega'' = \omega + \omega'$ is approximately satisfied.

Since the formal expansion scheme is standard, we briefly present the equation at each order starting from the nonlinear ion gyrokinetic equation.⁹ The electron nonlinearity is taken to be small since the characteristic phase velocity of these fluctuations is slow relative to the electron thermal

velocity. The nonlinear gyrokinetic equation is

$$(\partial_t + v_{\parallel} \mathbf{b} \cdot \nabla) g + i[\omega\tau + \omega_{*e}\{1 + (u^2 - 3)\eta_i/2\}] \phi_{\mathbf{k}} J_0 F_m = \nabla \psi J_0 \times \mathbf{b} \cdot \nabla g, \quad (8)$$

where g is the nonadiabatic part of the perturbed distribution function; i.e.,

$g = f_1 + F_m e^{\phi/T_i}$, $F_m = n_0 (M_i/2\pi T_i)^{3/2} \exp(-u^2/2)$, $u^2 = M_i v^2/T_i$, $\mathbf{b} = \mathbf{B}/|\mathbf{B}|$, and $J_0(k_{\perp} \rho_i)$ is a Bessel function.

We begin our analysis of Eq.(8) by noting that the right side represents the $\mathbf{E} \times \mathbf{B}$ convective nonlinearity. This term is assumed to be smaller than the linear terms in weak turbulence theory. To the dominant order, the test mode at \mathbf{k} obeys the linear relation.

$$L_{\mathbf{k}}^{-1} g_{\mathbf{k}}^{(1)} = -i[\omega\tau + \omega_{*e}\{1 + (u^2 - 3)\eta_i/2\}] \phi_{\mathbf{k}} J_0 F_m, \quad (9)$$

where $L_{\mathbf{k}} = i(\omega - k_{\parallel} v_{\parallel} + i0^+)^{-1}$ is the linear test particle propagator. To the next order, the mode at shorter wavelength \mathbf{k}^* is driven by the nonlinear interaction of the test mode at \mathbf{k} and the background modes at \mathbf{k}' ; i.e.,

$$L_{\mathbf{k}^*}^{-1} g_{\mathbf{k}^*}^{(2)} - \nabla \phi_{\mathbf{k}} J_0 \times \mathbf{b} \cdot \nabla g_{\mathbf{k}}^{(1)} - \nabla \phi_{\mathbf{k}'} J_0 \times \mathbf{b} \cdot \nabla g_{\mathbf{k}}^{(1)} = 0, \quad (10)$$

where $\mathbf{k}^* = \mathbf{k} + \mathbf{k}'$. The "induced potential" $\phi_{\mathbf{k}^*}^{(2)}$ is obtained by imposing the quasineutrality condition at the second order.

$$\epsilon^{(1)}(\omega^*, \mathbf{k}^*) \phi_{\mathbf{k}^*}^{(2)} = -i(\mathbf{k} \times \mathbf{k}' \cdot \mathbf{b}) \phi_{\mathbf{k}} \phi_{\mathbf{k}'} \{(\omega_{*e}/\omega_{\mathbf{k}}) - (\omega_{*e}'/\omega_{\mathbf{k}'})\} \\ \int d^3 u [J_0 J_0' J_0^* \{1 + (u^2 - 3)\eta_i/2\} / (\omega^* - k_{\parallel} v_{\parallel} + i0^+)] F_m, \quad (11)$$

where $J_0 = J_0(k_{\perp} \rho_i)$, $J_0' = J_0(k'_{\perp} \rho_i)$, and $\epsilon^{(1)}(\omega^*, \mathbf{k}^*) = 1 + k_y^{-2} \rho_s^2 - (\omega_{*e}^*/\omega_{\mathbf{k}^*}) \times \{1 - b_y^*(1 + \eta_i)\}$ is the local expression for the linear dielectric function. To the third order, the back reaction of the driven modes on the test mode gives the nonlinear correction to the distribution function at \mathbf{k} ; i.e.,

$$L_{\mathbf{k}}^{-1} g_{\mathbf{k}}^{(3)} = -\sum_{\mathbf{k}'} (\mathbf{k}' \times \mathbf{k}^* \cdot \mathbf{b}) \{ \phi_{\mathbf{k}'} (g_{\mathbf{k}^*}^{(2)} - i L_{\mathbf{k}^*}^{-1} [\omega\tau + \omega_{*e}\{1 + (u^2 - 3)\eta_i/2\}] \phi_{\mathbf{k}^*}) J_0' \\ - \phi_{\mathbf{k}^*}^{(2)} g_{\mathbf{k}'}^{(1)} J_0^* \}. \quad (12)$$

Hereafter, the first term on the right side of Eq.(11) will be referred to as

the "bare" contribution, because this distribution function response is directly driven through the nonlinear interaction of $\phi_{\mathbf{k}}$ with $\phi_{\mathbf{k}'}$ as described in Eq.(10). The remaining two terms will be referred to as the "shielding" contribution since these are due to the $\phi_{\mathbf{k}}^{(2)}$ fluctuation self-consistently induced by $g_{\mathbf{k}}^{(2)}$. Physically, the "bare" contribution represents the ion Compton scattering; i.e., the transit interaction of the ion with the beat wave at the phase velocity, $(\omega+\omega')/(k_{\parallel}+k'_{\parallel})$. The "shielded" contribution includes both the coherent 3-mode coupling and the "induced scattering" effects. The coherent mode coupling is associated with the distribution function response which is proportional to $\phi_{\mathbf{k}}$. Other "incoherent" mode coupling terms (which are not proportional to $\phi_{\mathbf{k}}$) are ignored. This is justified here because such terms would require finite amplitudes for both $\phi_{\mathbf{k}'}$ and $\phi_{\mathbf{k}}^{(2)}$. Given the fact that the threshold for negative η_i modes is higher for the higher k modes, this contribution is negligible since the amplitude of $\phi_{\mathbf{k}}^{(2)}$ is very small. The "induced scattering" is similar to the ion Compton scattering in the sense that both processes are nonlinear wave-particle interactions. The difference is that the induced scattering involves the interaction with a nonlinearly produced 'virtual mode' instead of an eigenmode. The Feynman diagrams for the aforementioned nonlinear processes as well as for the linear wave-particle interaction (Landau damping) are plotted in Fig.2. Finally, by requiring quasineutrality up to third order, we obtain the formal nonlinear eigenmode equation.

$$\begin{aligned}
 (1+\tau^{-1})\phi_{\mathbf{k}} - \int d^3v (-iL_{\mathbf{k}}^{-1}) J_0^2 [\omega\tau + \omega_e \{1 + (u^2 - 3)\eta_i / 2\}] F_m \phi_{\mathbf{k}} \\
 = \int d^3v J_0 g_{\mathbf{k}}^{(3)}. \tag{13}
 \end{aligned}$$

Here, the first two terms on the left side are from the adiabatic responses

of electrons and ions, respectively. The third term is the nonadiabatic ion linear response, and the right side represents the nonlinear response.

Up to this point in this section, we have not adopted any linear frequency orderings with respect to the ion transit frequency. This has allowed us to retain the general characteristics of the various nonlinear processes in the analysis. Having identified the relevant nonlinear processes in Eq.(12) and Fig.2, we can now proceed to simplify the analysis based on our knowledge of the linear mode structure and eigenfrequency. As shown in Ref.7, the real frequency of the mode is typically much greater than the ion transit frequency for most of the relevant regime where the fluctuation amplitude is finite; i.e., the mode is well-localized within the ion Landau resonance point ($x_i = L_S |\omega| / k_y v_{ti}$). After adopting the frequency ordering of $\omega \gg k_{\parallel} v_{ti}$, Eq.(13) simplifies to

$$\begin{aligned} & \{[(1+(1+\eta_i)/\Omega\tau) - (1+(1+2\eta_i)/\Omega\tau)3b_y/2] \partial_x^2 + Q_L(X)\} \phi_k \\ & = -\sum_{\mathbf{k}'} (\omega\omega')^{-1} (\mathbf{k}\times\mathbf{k}'\cdot\mathbf{b})^2 \{(\omega_{*e}/\omega_{\mathbf{k}}) - (\omega_{*e}'/\omega_{\mathbf{k}'})\} \langle J_0^2 J_0'^2 \{1+(u^2-3)\eta_i/2\} \rangle \\ & \quad - \epsilon^{(1)}(\omega^*, \mathbf{k}^*)^{-1} \{(\omega_{*e}'/\omega_{\mathbf{k}'}) - (\omega_{*e}''/\omega_{\mathbf{k}''})\} \langle J_0 J_0' J_0'' \{1+(u^2-3)\eta_i/2\} \rangle^2 \\ & \quad - \langle J_0 J_0' J_0'' \{1+(u^2-3)\eta_i/2\} \rangle^2 / \{1 - (1-\Gamma_0(b^*)) (1+\eta_i)\} |\phi_{\mathbf{k}'}|^2 \phi_{\mathbf{k}}. \quad (14) \end{aligned}$$

where $Q_L(X) = \{1/\Omega - 1 - \tau b_y (1+(1+\eta_i)/\Omega)\} + \{(1+(1+\eta_i)/\Omega\tau) - (1+(1+2\eta_i)/\Omega\tau) b_y\} (L_{\parallel}/L_S)^2 (X/\Omega)^2$, and $\langle \dots \rangle$ is the average over the velocity space. In Eq.(14), we have rearranged the last two terms on the right side in order to facilitate the following discussions about the dominant nonlinear saturation mechanism. The first and second terms represent, respectively, the approximated ion Compton scattering and coherent 3-mode coupling effects. The last term on the right side is the induced scattering which comes from the low frequency virtual mode contribution to $\epsilon^{(1)}$. We note that for the

parameter regime considered, the 3-mode coupling term is dominant due to the following reasons:

(i) Although there exists a finite dispersion ($\partial\Omega/\partial k_y \neq 0$), this is due to a small finite Larmor radius correction ($\propto b$). Hence, since the frequency mismatch is small, $\epsilon^{(1)}(\omega^*, k^*)$ is approximately resonant and the 3-mode coupling term would be large.

(ii) There are large cancellations between the ion Compton scattering and the induced scattering terms in the moderately long wavelength regime of interest in the present work. The magnitude of the remaining term would be of order b^2 which is smaller than the 3-mode coupling term by order b . The details of this calculation are presented in the Appendix.

By keeping only the dominant 3-mode coupling contribution to the nonlinear eigenmode equation, we obtain

$$[\{ (1 + (1 + \eta_i)/\Omega\tau) - (1 + (1 + 2\eta_i)/\Omega\tau) 3b_y/2 \} \partial_X^2 + Q_L(X) + Q_{NL}(X)] \phi_k = 0, \quad (15)$$

where $Q_L(X)$ is defined following Eq.(14) and

$$Q_{NL}(X) = \sum_{k'} (\omega\omega^*)^{-1} (k \times k' \cdot b)^2 \{ (\omega_{*e}/\omega_k) - (\omega_{*e}'/\omega_{k'}) \} \times \epsilon^{(1)}(\omega^*, k^*)^{-1} \{ (\omega_{*e}'/\omega_{k'}) - (\omega_{*e}/\omega_k) \} \langle J_0 J_0' J_0^* \{ 1 + (u^2 - 3)\eta_i/2 \} \rangle^2 |\phi_{k'}|^2.$$

We note that the imaginary part of the nonlinear potential acts effectively as a nonlinear damping on the test mode via energy transfer to shorter wavelength modes. In a sheared slab geometry with multi-rational surfaces, the $Q_{NL}(X)$ can be approximated by $Q_{NL}(0)$, since significant energy transfer to ions can occur through background modes k' at $X=0$ due to the finiteness of X' . By solving Eq.(15) for Ω and treating $\text{Im}Q_{NL}(0)$ as a given quantity, we obtain

$$\gamma_{NL} = \gamma_L - |\omega_{*e}| \text{Im}Q_{NL}(0). \quad (16)$$

This describes a competition between the linear growth and the nonlinear transfer which acts as an effective damping on the test mode. Nonlinear saturation of instability occurs when these two processes balance.

IV. Saturated Fluctuations and Associated Thermal Transport

In this section, we derive the saturation levels of various fluctuations and the associated ion thermal diffusivity. The analysis that follows demonstrates that these quantities vanish at the threshold. As noted before, a naive extrapolation of the mixing length formula to the regime near threshold does not show this apparent behavior.⁶

In Eq.(16), the right side depends on the spectral summation of various modes. One way of evaluating such a discrete sum is to approximate it with an integral. However, such a procedure¹⁰ still produces a complicated integral equation which cannot be solved without making many further crude approximations. A simpler method which is equally reliable, is to estimate the spectral sum in terms of the basic characteristic scalings and various spectrum-averaged rms (root-mean-squared) values. This approximation is well-justified here because only the moderately long wavelength modes are linearly excited. Recall from Sec.II that the shorter wavelength modes are damped due to their higher thresholds. Also, the extremely long wavelength modes are subdominant when properly considered in the context of the fluid description with strong ion-ion collisions.¹⁹ Therefore, the range of the spectrum which is strongly excited is rather

narrow.

Noting the fact that the 3-wave decay type resonance condition is approximately satisfied due to finite dispersion, we make the following approximation in $\text{Im}Q_{\text{NL}}(0)$; i.e.,

$$\text{Im}[\epsilon^{(1)}(\omega^*, k^*)^{-1}] = |\partial\epsilon^{(1)}/\partial\omega^*|^{-1} \delta\omega / \{\delta\omega^2 + (\omega^* - \omega' - \omega)^2\}. \quad (17)$$

Then, by using Eqs. (16) and (17) for $\text{Im}Q_{\text{NL}}(0)$ and the radial mode-width, $\Delta = |L_S \Omega / L_n|^{1/2}$, for k_r^{-1} , we obtain

$$[\phi\psi/T_i]_{\text{rms}} = (\Delta/L_n)(\sigma/\delta\omega)^{1/2} = J(\eta_i, b_y)\rho_i/L_n. \quad (18)$$

and similarly,

$$[\delta T_i/T_i]_{\text{rms}} = (\Delta/L_T)(\sigma/\delta\omega)^{1/2} = J(\eta_i, b_y)\rho_i/L_T. \quad (19)$$

where

$$J = (1 - 5b_y/2)^{1/2} [b_y \{1 - b_y(1 + \eta_i)\}]^{-1/2} \\ \{ |(\eta_i - \eta_{c1})(\eta_i - \eta_{c2})|^{1/2} / |1 + \tau + \eta_i| \}^{1/2}, \text{ for } \eta_i < \eta_{c2}.$$

Finally, the ion thermal diffusivity can be obtained from the quasilinear conduction contribution to the ion thermal flux, Q_i ; i.e.,

$$Q_i = \text{Im} \sum_{\mathbf{k}} [c k_y \phi \delta T_i / B_0]. \quad (20a)$$

and

$$\chi_i = -Q_i L_T / T_i = [(\sigma/\omega^2) c^2 k_y^2 |\phi|^2 / B_0^2]_{\text{rms}} = [\sigma^2 \Delta^2 / \delta\omega] \\ = I(\eta_i, b_y) |c T_i / e B_0| \rho_i / L_S. \quad (20b)$$

where $I = \pi^{-1} (1 - 5b_y/2)^2 [(1 + b_s) \{1 - b_y(1 + \eta_i)\}]^{-1}$

$$\{ |(\eta_i - \eta_{c1})(\eta_i - \eta_{c2})| / |1 + \tau + \eta_i| \}. \text{ for } \eta_i < \eta_{c2}. \quad (20c)$$

It is important to point out that the saturation levels for the fluctuations and their associated thermal diffusivities derived here are considerably smaller than strong turbulence estimates for these quantities. Note that they vanish at the threshold η_{c2} , and near marginal stability, $\chi_i \propto$

$|\eta_i - \eta_{c2}|$, while $e\phi/T_i$, $\delta T_i/T_i \propto |\eta_i - \eta_{c2}|^{1/4}$. Therefore, the onset of ion-temperature-gradient-driven turbulence associated with negative η_i -modes is predicted to be more abrupt near the threshold than the positive η_i mode cases.¹⁰ On the other hand, away from the threshold (as $|L_n|$ is increased), the turbulence level and thermal diffusivity remain small. This fact is summarized in Fig.3 where χ_i , $\delta T_i/T_i$ and $e\phi/T_i$ are plotted as functions of $|L_n|$ with other parameters fixed. Here, we should not expect to observe a dramatic confinement degradation in experiments where the density profile becomes flatter (provided their instability threshold has already been exceeded).

V. Discussion

In this paper, a weak turbulence theory of η_i modes is presented which is applicable to the inverted density profile cases characteristics of numerous H-mode discharges in JET^{1,2} and DIII-D.³ Our results indicate that both the saturation level for the negative- η_i -mode fluctuations and the magnitude of the associated ion thermal diffusivity are considerably smaller than the familiar strong turbulence mixing-length type estimates for the conventional positive- η_i -instabilities.

The dominant nonlinear saturation mechanism is the coherent mode coupling to shorter wavelength modes. This is because the longer wavelength modes are more easily excited due to their lower instability thresholds, and the combined effects of the ion Compton scattering and the induced scattering are negligible in the long wavelength regime. This has made our

radially nonlocal analysis possible in the context of the usual differential approximation. However, in the case of positive- η_i -modes considered in Ref.10, the shorter wavelength instabilities are more easily excited due to their lower thresholds, and the ion Compton scattering is the dominant nonlinear process. In this short wavelength regime, the radially nonlocal analysis is extremely difficult to implement since the differential approximation breaks down.

As a final note, we discuss the possibility of applying the weak turbulence type theory developed here to the case of flat density profile plasmas, which are also observed in the H-mode discharges of various tokamaks. In this case, the stability threshold is approximately given by $L_S/L_{Ti} = 3.8$ for the slab η_i mode,⁷ and by $R/L_{Ti} = 3.0$ for the interchange-like toroidal η_i mode.^{6,8} Although such thresholds appear to be exceeded for typical H-mode profiles, they could be significantly affected by more complicated realistic effects not considered in these theoretical studies. If such modifications (e.g., impurities, finite beta, etc.) led to the conclusion that the longer wavelength modes are more easily excited, we would expect that the 3-wave-decay type nonlinear process would be the dominant nonlinear saturation mechanism, as indicated by the results of the present work. This would accordingly suggest that many features in the present paper could be applied to the weak turbulence theory of the flat density ion temperature gradient modes.

Acknowledgments

The authors gratefully acknowledge useful discussions with L. Chen, P. H. Diamond, B. G. Hong, J. A. Krommes, and N. Mattor.

This work is supported by U.S. Department of Energy Contract No. DE-AC02-76-CHO3073.

**Appendix: Cancellation between ion Compton scattering
and induced scattering terms**

Here, we evaluate the various nonlinear coupling integrals in the long wavelength limit to demonstrate the near-cancellation between the ion Compton scattering and the induced scattering terms. From Eq.(14), the ion Compton scattering term is governed by the integral,

$$I_C = \langle J_0^2 J_0'^2 \{1 + (u^2 - 3)\eta_i/2\} \rangle \\ = \int_0^\infty du u J_0^2(b^{1/2}u) J_0'^2(b^{1/2}u) \{1 + (u^2 - 2)\eta_i/2\} \exp(-u^2/2), \quad (A1)$$

where the trivial $v_{||}$ integration has already been performed. Expanding the Bessel functions in the small argument limit and defining $x = u^2/2$, we obtain

$$I_C = \int_0^\infty dx e^{-x} (1 - bx)(1 - b'x)(1 - \eta_i + \eta_i x) + O(b^2) \\ = 1 - (1 + \eta_i)(b + b') + O(b^2), \quad (A2)$$

where $b' \sim b$ has been assumed. The induced scattering contribution in Eq.(14) is governed by the integral,

$$I_i = \langle J_0 J_0' J_0'' \{1 + (u^2 - 3)\eta_i/2\} \rangle \\ = \int_0^\infty du u J_0(b^{1/2}u) J_0'(b^{1/2}u) J_0''(b^{1/2}u) \{1 + (u^2 - 2)\eta_i/2\} \exp(-u^2/2). \quad (A3)$$

Again, expanding the Bessel functions, we obtain

$$I_i = \int_0^\infty dx e^{-x} (1 - bx/2)(1 - b'x/2)(1 - b''x/2)(1 - \eta_i + \eta_i x) + O(b^2) \\ = 1 - (1 + \eta_i)(b + b' + b'')/2 + O(b^2), \quad (A4)$$

where $b' \sim b \sim b''$ has been assumed again. Finally, using the results from Eqs. (A2) and (A4) with Eq.(14), we show that the combined effect of the ion Compton scattering processes and the induced scattering processes is

proportional to,

$$\begin{aligned} I_c &= I_i^2 / \{1 - (1 - \Gamma_0(b^*)) (1 + \eta_i)\} \\ &= \{1 - (1 + \eta_i)(b + b')\} - \{1 - (1 + \eta_i)(b + b' + b^*)/2\}^2 / \{1 - (1 - \Gamma_0(b^*)) (1 + \eta_i)\} \\ &+ O(b^2) = O(b^2). \end{aligned} \tag{A5}$$

Equation (A5) illustrates the fact that the combined effect of ion Compton scattering and the induced scattering processes cancel up to order b . The remainder is order b^2 , and smaller than the 3-wave coupling term (retained in the nonlinear analysis of Sec.III) by order b .

References

- 1 C. Gowers, D. Barlett, A. Boileau, S. Corti, A. Edwards, N. Gottardi, K. Hirsch, M. Keilhacker, E. Lazzaro, P. Morgan, P. Nielsen, J. O'Rourke, H. Salzmann, P. Smeulders, A. Tanga, and M. von Hellermann, in *Proceedings of the 15th European Conference on Controlled Fusion and Plasma Heating* (European Physical Society, Budapest, 1988), Vol. 12B, Part1, p. 2239.
- 2 P. Smeulders, N. Gottardi, E. Lazzaro, M. Brusati, B. Keegan, S. Howak, D. Pasini, F. Rimini, "Hollow Profiles and High Beta Effects During H-Modes in JET," Joint European Torus Report JET-IR(88) 11, January (1988).
- 3 D. P. Schissel, R. E. Stockdale, H. St. John, and W. M. Tang, *Phys. Fluids* **31**, 3738 (1988).
- 4 R. R. Dominguez and R. E. Waltz, *Phys. Fluids* **31**, 3147 (1988).
- 5 H. Biglari, P. H. Diamond, and M. N. Rosenbluth, *Phys. Fluids B* **1**, 109 (1989).
- 6 F. Romanelli, *Phys. Fluids B* **1**, 1018 (1989).
- 7 T. S. Hahm and W. M. Tang, *Phys. Fluids B* **1**, 1185 (1989).
- 8 R. R. Dominguez and M. N. Rosenbluth, *Nucl. Fusion*, **29**, 844 (1989).
- 9 E. A. Frieman and L. Chen, *Phys. Fluids* **25**, 502 (1982).
- 10 N. Mattor and P. H. Diamond, *Phys. Fluids B* (to be published).
- 11 W. M. Tang, R. B. White, and P. N. Guzdar, *Phys. Fluids* **23**, 167 (1980).
- 12 W. M. Tang, G. Rewoldt, and L. Chen, *Phys. Fluids* **29**, 3715 (1987).

- ¹³ B. Coppi, M. N. Rosenbluth, and R. Z. Sagdeev, *Phys. Fluids* **10**, 582 (1967).
- ¹⁴ R. E. Waltz, W. Pfeiffer, and R. R. Dominguez, *Nucl. Fusion* **20**, 43 (1980).
- ¹⁵ P. W. Terry, J. N. Leboeuf, P. H. Diamond, D. R. Thayer, J. E. Sedlak, and G. S. Lee, *Phys. Fluids* **31**, 2920 (1988).
- ¹⁶ W. M. Tang, N. L. Bretz, T. S. Hahm, W. W. Lee, F. W. Perkins, M. H. Redi, G. Rewoldt, M. C. Zarnstorff, S. J. Zweben, R. D. Sydora, J. M. Dawson, V. K. Decyk, H. Naitou, T. Kamimura, and Y. Abe, in *Plasma Physics and Controlled Fusion Research, 1988, Proceedings of the 12th International Conference, Nice (IAEA, Vienna, in press)*.
- ¹⁷ R. Z. Sagdeev and A. A. Galeev, in *Nonlinear Plasma Theory*, edited by T. M. O'Neil and D. L. Book (Benjamin, New York, 1969), pp. 103-111.
- ¹⁸ Liu Chen, R. L. Berger, J. G. Lominadze, M. N. Rosenbluth, and P. H. Rutherford, *Phys. Rev. Lett*, **39**, 754 (1977).
- ¹⁹ T. Antonsen, B. Coppi, and R. Englade, *Nucl. Fusion* **19**, 641 (1979).

Figures

FIG. 1. Plot of α , $\delta\omega$, and $|\alpha/\delta\omega|$ as functions of η_i

for $b_S = 0.16$, $L_T/L_S = 0.04$, $z = 1$.

- a. Plot of α from Eq. (6).
- b. Plot of $\delta\omega$.
- c. Plot of $|\alpha/\delta\omega|$ from Eq. (7a).

FIG. 2. Feynman diagrams for various physical processes. Wavy line and solid line represent the wave and particle, respectively. Dotted line corresponds to a virtual mode.

FIG. 3. Plot of predicted ion thermal diffusivity and fluctuation levels as functions of η_i for $b_S = 0.16$, $L_T/L_S = 0.04$, $z = 1$.

- a. Plot of χ_i from theoretical expression, Eq. (20c).
- b. Plot of $\delta T_i/T_i$ from theoretical expression, Eq. (19).
- c. Plot of $e\phi/T_i$ from theoretical expression, Eq. (18).

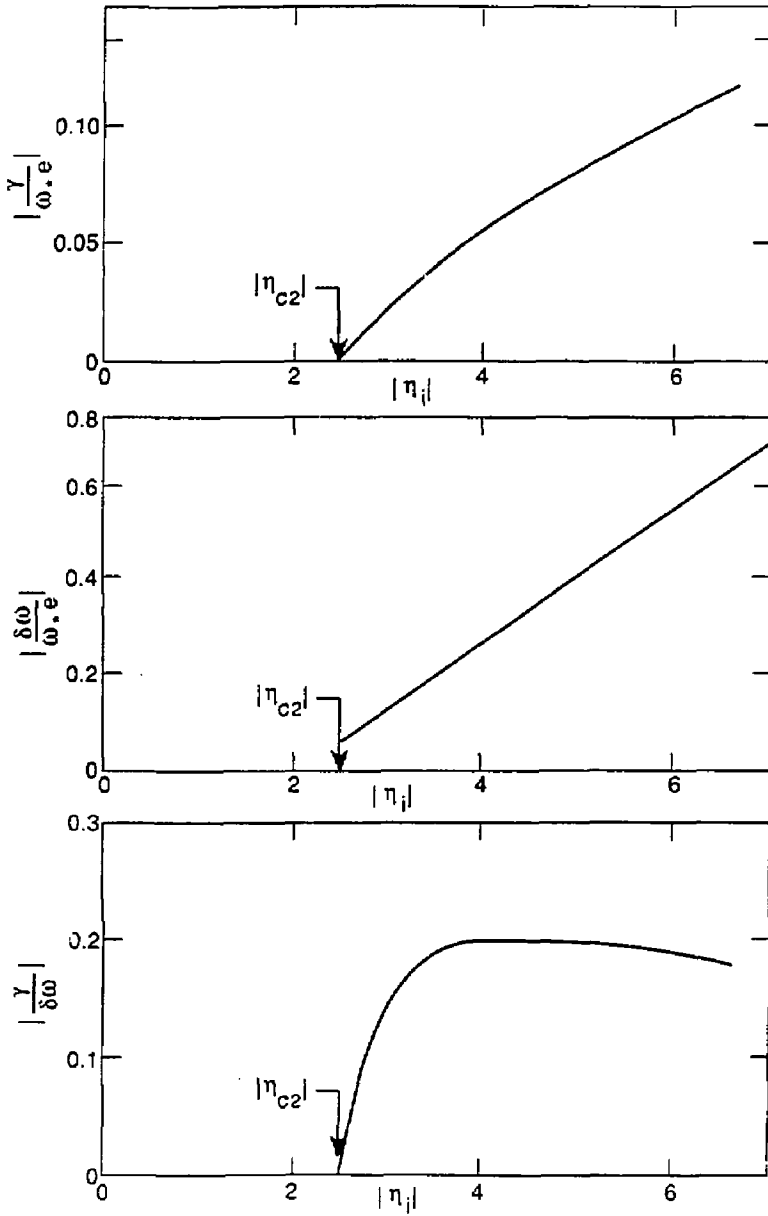


Fig. 1

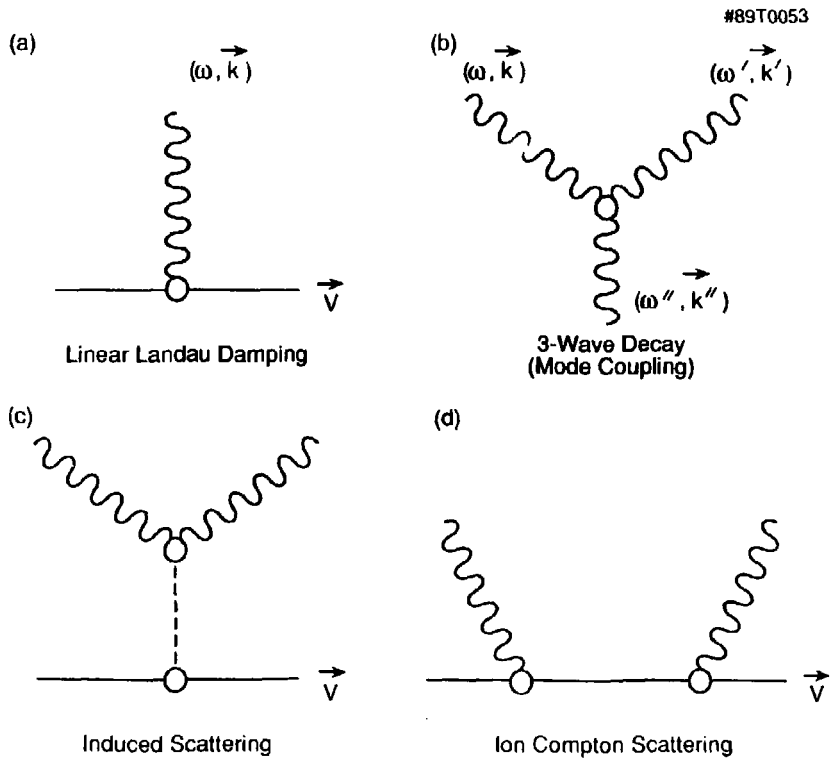


Figure 2

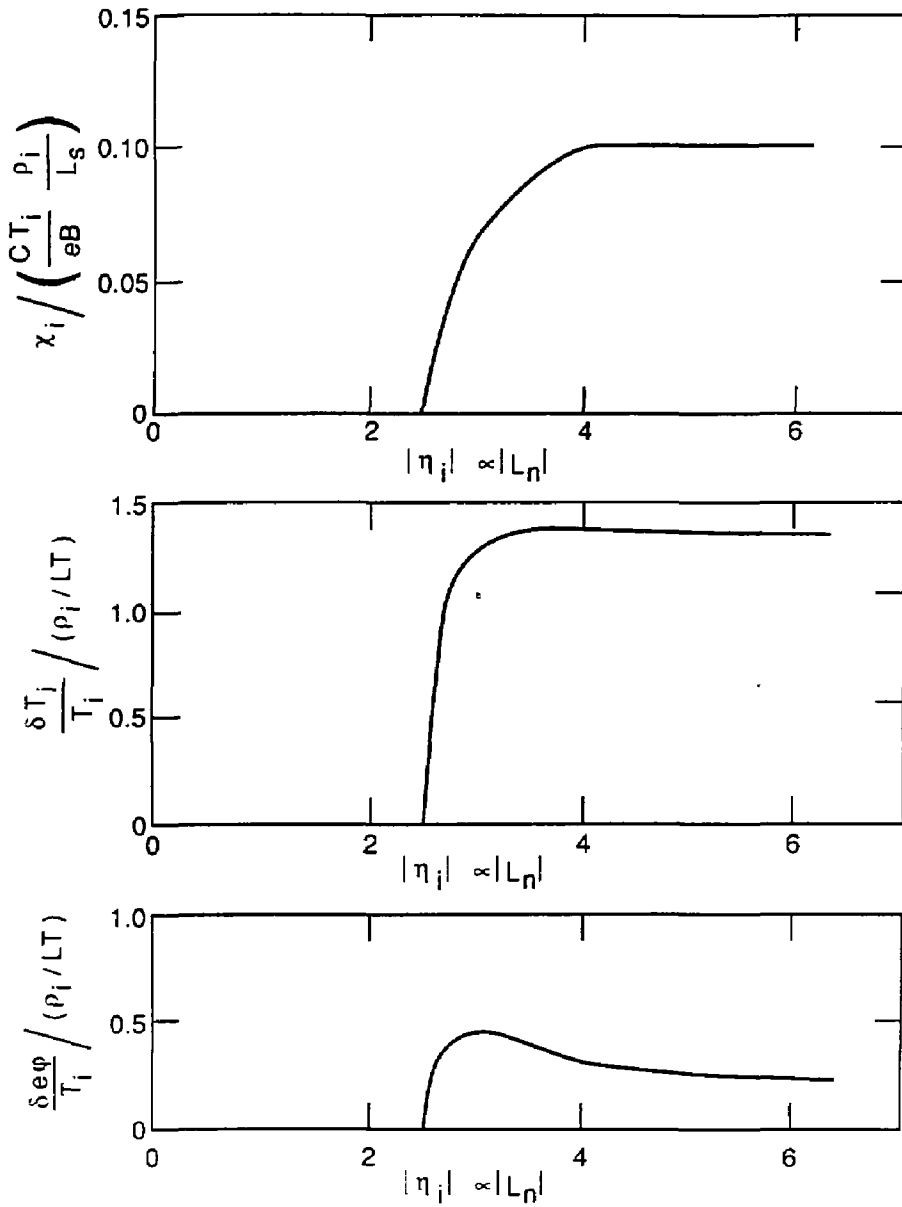


Fig. 3

EXTERNAL DISTRIBUTION IN ADDITION TO UC-420

Dr. Frank J. Paoloni, Univ of Wollongong, AUSTRALIA
Prof. M.H. Brennan, Univ Sydney, AUSTRALIA
Plasma Research Lab., Australian Nat. Univ., AUSTRALIA
Prof. I.R. Jones, Flinders Univ., AUSTRALIA
Prof. F. Cap, Inst Theo Phys, AUSTRIA
Prof. M. Heindler, Institut für Theoretische Physik, AUSTRIA
M. Goossens, Astronomisch Instituut, BELGIUM
Ecole Royale Militaire, Lab de Phys Plasmas, BELGIUM
Commission-European, Dg-XIII Fusion Prog, BELGIUM
Prof. R. Bouciqué, Rijksuniversiteit Gent, BELGIUM
Dr. P.H. Sakanaka, Instituto Física, BRAZIL
Instituto De Pesquisas Especiais-IMPÉ, BRAZIL
Documents Office, Atomic Energy of Canada Limited, CANADA
Dr. M.P. Bachynski, MPB Technologies, Inc., CANADA
Dr. H.M. Skarsgard, University of Saskatchewan, CANADA
Dr. H. Barnard, University of British Columbia, CANADA
Prof. J. Teichmann, Univ. of Montreal, CANADA
Prof. S.R. Sreenivasan, University of Calgary, CANADA
Prof. Tudor H. Johnston, INRS-Energie, CANADA
Dr. Bolton, Centre canadien de fusion magnétique, CANADA
Dr. C.R. James, Univ. of Alberta, CANADA
Dr. Peter Lukac, Komenského Univ, CZECHOSLOVAKIA
The Librarian, Culham Laboratory, ENGLAND
The Librarian, Rutherford Appleton Laboratory, ENGLAND
Mrs. S.A. Hutchinson, JET Library, ENGLAND
C. Mouttet, Lab. de Physique des Milieux Ionisés, FRANCE
J. Rader, CEN/CADARACHE - Bat 506, FRANCE
Ms. C. Rinni, Librarian, Univ. of Ioannina, GREECE
Dr. Tom Mual, Academy Bibliographic Ser., HONG KONG
Preprint Library, Hungarian Academy of Sciences, HUNGARY
Dr. B. Das Gupta, Saha Inst of Nucl. Phys., INDIA
Dr. P. Kaw, Institute for Plasma Research, INDIA
Dr. Philip Rosenau, Israel Inst. of Tech, ISRAEL
Librarian, Inst Theo Phys, ITALY
Prof. G. Rostagni, Istituto Gas Ionizzati Del CNR, ITALY
Mass Cella De Palo, Assoc EURATOM-ENEA, ITALY
Dr. G. Grosso, Istituto di Fisica del Plasma, ITALY
Dr. H. Yamato, Toshiba Res & Dev, JAPAN
Prof. T. Kawakami, Atomic Energy Res. Institute, JAPAN
Prof. Kyôji Nishikawa, Univ of Hiroshima, JAPAN
Director, Dept. Large Tokamak Res. JAERI, JAPAN
Prof. Satoshi Itoh, Kyushu University, JAPAN
Research Info Center, Nagoya University, JAPAN
Prof. S. Tanaka, Kyoto University, JAPAN
Library, Kyoto University, JAPAN
S. Mori, JAERI, JAPAN
H. Jeong, Librarian, Korea Advanced Energy Res Inst, KOREA
Dr. I. Choi, The Korea Adv. Inst of Sci & Tech, KOREA
Prof. B.S. Liley, University of Waikato, NEW ZEALAND
Institute of Plasma Physics, PEOPLE'S REPUBLIC OF CHINA
Librarian, Institute of Phys., PEOPLE'S REPUBLIC OF CHINA
Library, Tsing Hua University, PEOPLE'S REPUBLIC OF CHINA
Z. Li, Southwest Inst. Physics, PEOPLE'S REPUBLIC OF CHINA
Prof. J.A.C. Cabral, Inst Superior Tecnico, PORTUGAL
Dr. Octavian Petrus, AL I CUZA University, ROMANIA
Dr. Jean de Villiers, Fusion Studies, AEC, SO AFRICA
Prof. M.A. Hellberg, University of Natal, SO AFRICA
C.I.E.M.A.T., Fusion Div. Library, SPAIN
Dr. Lennart Stenflo, University of UMEA, SWEDEN
Library, Royal Institute of Tech, SWEDEN
Prof. Hans Wilhelmson, Chalmers Univ of Tech, SWEDEN
Centre Phys des Plasmas, Ecole Polytech Fed, SWITZERLAND
Bibliotiek, Fom-Inst Voor Plasma-Fysica, THE NETHERLANDS
Metin Durgut, Middle East Technical University, TURKEY
Dr. D.D. Ryutov, Siberian Acad Sci, USSR
Dr. G.A. Eliseev, Kurchatov Institute, USSR
Dr. V.A. Glukhikh, Inst Electrophysical Apparatus, USSR
Prof. O.S. Padichenko, Inst. of Phys. & Tech. USSR
Dr. L.M. Kovrzhnykh, Institute of Gen. Physics, USSR
Nuclear Res. Establishment, Julich Ltd., W. GERMANY
Bibliotek, Inst. Für Plasmavorschung, W. GERMANY
Dr. K. Schindler, Ruhr-Universität Bochum, W. GERMANY
ASDEX Reading Rm, c/o Wagner, IPP/Max-Planck, W. GERMANY
Librarian, Max-Planck Institut, W. GERMANY
Prof. R.K. Janev, Inst of Phys, YUGOSLAVIA